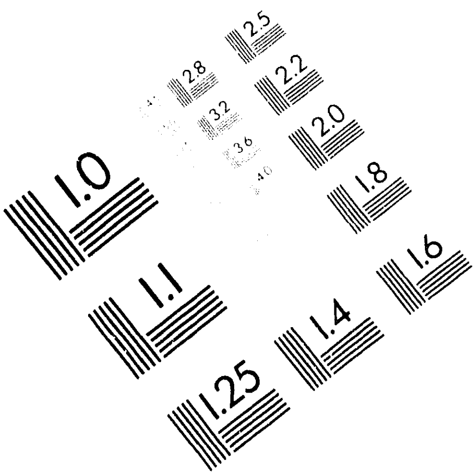
1.0
1.1
1.25
1.4
1.6
1.8
2.0
2.2
2.5
2.8
3.2
3.6

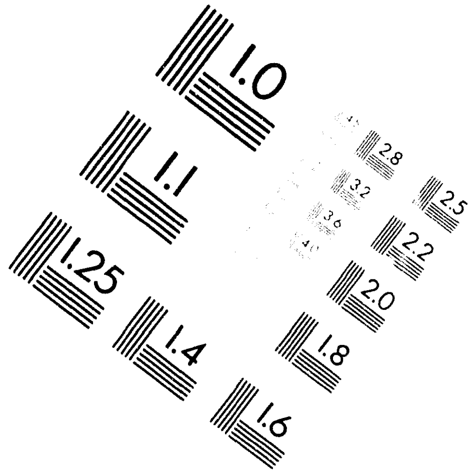
1.0
1.1
1.25
1.4
1.6
1.8
2.0
2.2
2.5
2.8
3.2
3.6

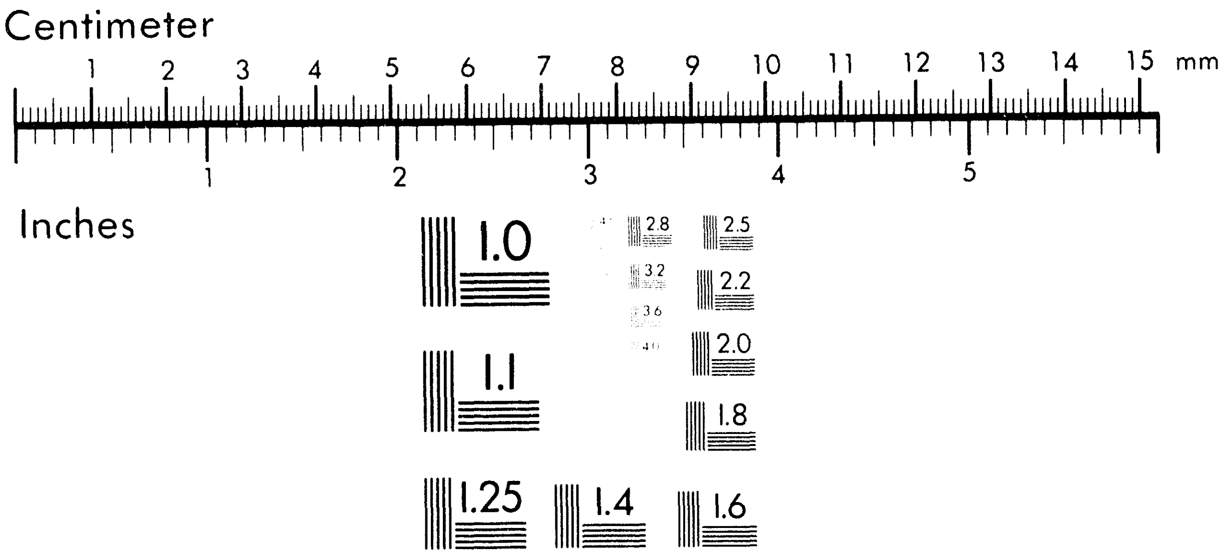
Centimeter
1
2
3
4
5
6
7
8
9
10
11
12
13
14
15
mm
1
2
3
4
5
Inches
1.0
2.8
2.5
3.2
2.2
3.6
2.0
1.1
1.8
1.25
1.4
1.6

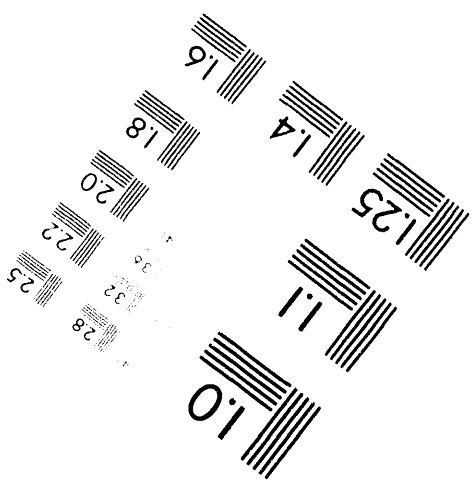
1.0
1.1
1.25
1.4
1.6
1.8
2.0
2.2
2.5
2.8
3.2
3.6

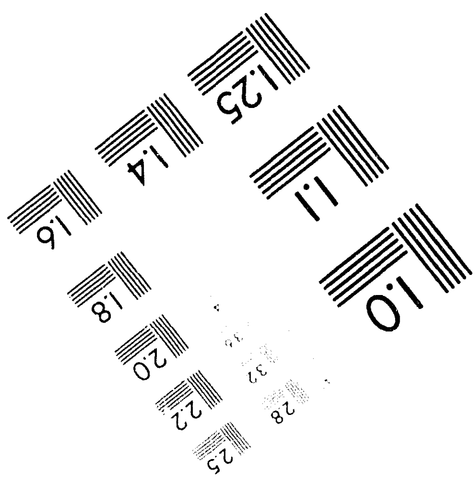
1.0
1.1
1.25
1.4
1.6
1.8
2.0
2.2
2.5
2.8
3.2

1 of 1

2

Conf-9308122--18

Mechanical behavior and phase stability of NiAl-based shape memory alloys

E. P. George,[1] C. T. Liu,[1] J. A. Horton,[1] H. Kunsmann,[2] T. King,[2] and M. Kao[3]

[1]Metals and Ceramics Division, Oak Ridge National Laboratory, Oak Ridge, TN 37831-6093
[2]Eaton Corporation, 4201 North 27th Street, Milwaukee, WI 53216
[3]Johnson Controls Inc., 1701 W. Civic Drive, Mail Stop A37, Milwaukee, WI 53209

NiAl-based shape memory alloys (SMAs) can be made ductile by alloying with 100-300 wppm B and 14-20 at.% Fe. The addition of Fe has the undesirable effect that it lowers the temperature (A_p) of the martensite→austenite phase transformation. Fortunately, however, A_p can be raised by lowering the "equivalent" amount of Al in the alloy. In this way a high A_p temperature of ~190°C has been obtained without sacrificing ductility. Furthermore, a recoverable strain of 0.7% has been obtained in a Ni-Al-Fe alloy with A_p temperature of ~140°C. Iron additions do not suppress the aging-induced embrittlement that occurs in NiAl alloys at 300-500°C as a result of Ni_5Al_3 precipitation. Manganese additions (up to 10 at.%) have the effect of lowering A_p, degrading hot workability, and decreasing room-temperature ductility.

INTRODUCTION

Off-stoichiometric NiAl alloys, with compositions in the range 61~65 at.% Ni, undergo a thermoelastic B2→$L1_0$ (martensite) phase transformation upon quenching from elevated temperatures [1-10]. Depending on the Ni/Al ratio, the martensite start (M_s) temperature of this transformation can be as high as 500°C [11,12]. These alloys, therefore, have the potential to be developed as high-temperature SMAs. However, binary NiAl alloys are quite brittle at ambient temperatures [13-15], and ways need to be found to improve their ductility. In this paper, we first summarize highlights of our recent alloy design efforts aimed at improving the ductility of NiAl-based SMAs. Our approach consisted of adding B and Fe—for enhanced grain boundary cohesion and improved cleavage resistance, respectively. Next, we discuss aging effects and the dependence of transformation temperatures on the Ni/Al ratio, and the Fe, Mn contents of NiAl-based alloys. We end with a discussion of tensile strain recoveries in Ni-Al-Fe-B alloys. Because of length limitations, we are unable to go into all the details here; rather, our goal is to merely highlight some of the significant results.

EXPERIMENTAL

All the alloys examined in this study contained Ni, Al, and Fe (in varying amounts) as the base constituents. In addition, depending on the alloy composition, 100 or 300 wppm B was added to each alloy to improve grain boundary cohesion. Some of the alloys contained small amounts (2–10 at.%) of Mn, which was added in an attempt to increase the M_s temperature. All the alloys were arc melted and drop cast into Cu chill molds. Following this they were clad in stainless steel and hot rolled at 1000°C in steps of 20% reduction in thickness per pass to a final thickness of 1.3~1.9 mm. The rolled sheets were annealed for 0.5 h in flowing argon gas at 1300°C and then quenched into an oil bath maintained at room temperature. The resulting microstructures were examined by standard metallographic techniques as well as X-ray diffraction. Differential scanning calorimetry (DSC) was used to study the various phase transformations taking place in these alloys at temperatures to 450°C. Tensile tests were carried out in ambient air at an engineering strain rate of 3.3 × 10^{-3} s^{-1}.

RESULTS AND DISCUSSION

As discussed in our earlier paper [2], and shown in Table 1, Fe contents of at least 14 at.% are needed to get adequate ductility in NiAl-based alloys. The probable reason for this is that increasing amounts of a ductile second phase form with increasing amounts of Fe in the alloy [2], and a minimum volume fraction of this second phase appears necessary to get adequate ductility. In general, the ductile alloys in Table 1 contain three phases—martensite, retained B2, and $L1_2$—with the relative amounts of each depending on the exact alloy composition (Fig. 1). Although we have not yet correlated the phases present in each of our alloys with their respective ductilities, our current speculation (based on Table 1 and Fig. 1) is that, in general, increased ductilities go hand in hand with increased amounts of the $L1_2$ phase.

Having investigated the ductility in the as-quenched state, we next investigated the dependence of ductility on aging treatments at elevated temperatures. As shown in Fig. 2, the ductility of SMA-23 drops dramatically after relatively short exposures at temperatures of 400-500°C (T > A_f). The principal reason for this appears to be precipitation of the embrittling Ni_5Al_3 phase in this temperature range,

"The submitted manuscript has been authored by a contractor of the U.S. Government under contract No. DE-AC05-84OR21400. Accordingly, the U.S. Government retains a nonexclusive, royalty-free license to publish or reproduce the published form of this contribution, or allow others to do so, for U.S. Government purposes."

DISCLAIMER

as demonstrated by the X-ray diffraction patterns in Fig. 3, which were taken at room temperature after 1-h exposures at the indicated temperatures. Clearly, future alloy design efforts should attempt to suppress this phase transformation, and the attendant aging-induced embrittlement, because not only are as-quenched ductilities important, but also ductilities after extended service exposures. In addition, future research should also investigate the kinetics of Ni_5Al_3 formation at lower temperatures (i.e., $T < A_s$), because it is possible that the martensite$\rightarrow Ni_5Al_3$ transformation proceeds even more rapidly than the $B2\rightarrow Ni_5Al_3$ phase transformation.

Table 1 Chemical compositions (at.%) and room-temperature tensile elongations of Ni-Fe-Al-B alloys.

Alloy	Ni	Al	Fe	Ductility
SMA-9	64.5	31.5	4.0	v. Brittle
SMA-11	63.7	28.3	8.0	Brittle
SMA-13	61.5	26.5	12.0	Brittle
SMA-15	59.0	27.0	14.0	Slight Duct.
SMA-23	58.5	25.5	16.0	7.0
SMA-33	57.8	25.1	17.1	6.6
SMA-48	58.1	24.8	17.1	8.4
SMA-26	57.3	24.6	18.1	8.4
SMA-17	56.1	23.9	20.0	12.0

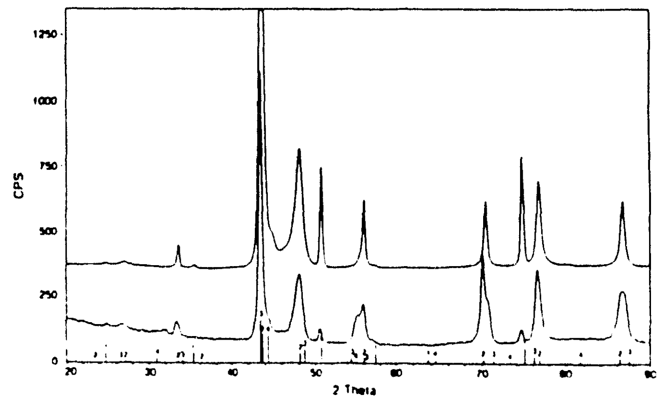

Fig. 1 X-ray diffraction spectra showing phases present in as-quenched SMA-48 (top) and SMA-23 (bottom). ($1 = L1_2$; 2 = martensite; $3 = Ni_5Al_3$; and 4 = B2.)

Next, we address the effect of Fe on the martensite$\rightarrow$B2 phase transformation in Ni-Al-Fe alloys. Unfortunately, as shown in Fig. 4, the addition of Fe decreases the transformation temperatures (defined for purposes of this discussion as the Austenite-peak, or A_p, temperatures). Note that the quantity Al_{eq} (= Al + ½Fe) in Fig. 4 is the "equivalent" amount of Al in the ternary Ni-Al-Fe alloys—assuming that Fe substitutes equally for the Ni and Al sites. While not quite rigorous, this treatment provides a simple framework for treating ternary Ni-Al-Fe alloys by analogy to their binary Ni-Al counterparts. The main conclusions to be drawn from Fig. 4 are that (*i*) A_p generally decreases with increases in both Fe concentration and Al_{eq}, and (*ii*) A_p is relatively insensitive to Fe concentration in the range 16-18 at.% Fe. So, for our next series of Ni-Al-Fe alloys, we fixed the Fe concentration at 17.1 at.% and varied Al_{eq} systematically. The results are plotted in Fig. 5, and show that A_p decreases systematically with increasing Al_{eq}. This is reminiscent of the decrease in M_s temperature with increasing Al content in binary NiAl alloys. Moreover, the slope in Fig. 5 (120°C/at.% Al_{eq}) is identical to that reported by Smialek and Hehemann [12] for the dependence of M_s temperature on Al concentration in binary NiAl alloys (120°C/at.% Al). It is also in reasonably good agreement with the slope (175°C/at.% Al) reported by Au and Wayman [11] for binary NiAl. An interesting point to note in Fig. 5 is that A_p appears to flatten out at around 190°C for $Al_{eq} < 33.4$ at.%. If this behavior is borne out by additional experiments, it may have technological significance because of the usefulness of operating in a composition range where the transformation temperatures are not overly sensitive to composition.

Since Mn is believed to increase the M_s temperature of NiAl alloys, our next step involved replacing the Fe in Ni-Al-Fe alloys with up to 10 at.% Mn. However, as shown in Fig. 6, Mn appeared to lower (not raise) the A_p temperature, at least at low Mn concentrations. While there is some indication that the curve begins to turn upwards at higher Mn concentrations, Mn has the deleterious effect that it degrades both hot workability and room temperature ductility. Therefore, it is not very attractive as a potential alloying element to raise the transformation temperatures of Ni-Al-Fe SMAs.

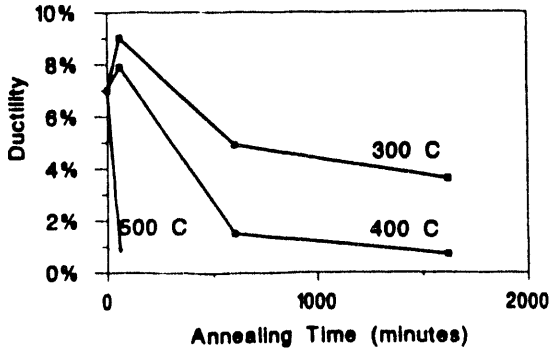

Fig. 2 Effect of aging treatment on room-temperature tensile ductility of SMA-23.

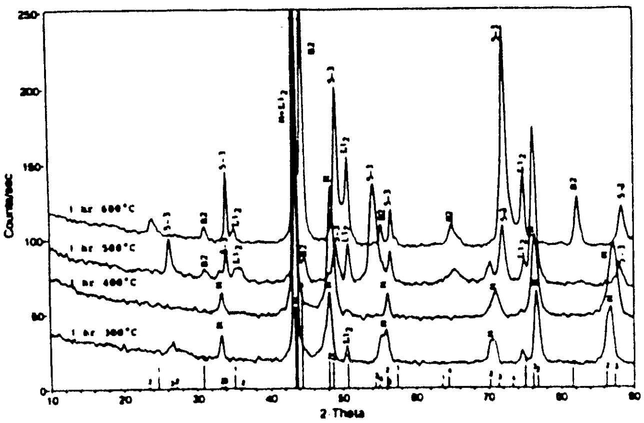

Fig. 3 X-ray diffraction spectra showing phases present in SMA-23 after indicated anneals. ($1 = L1_2$; $2 =$ martensite; $3 = Ni_5Al_3$; and $4 =$ B2.)

Finally, we address the issue of strain recovery in one of our alloys, SMA-23. A sheet tensile specimen of this alloy was annealed for 0.5 h at 1300°C and oil quenched to get the martensite structure (Fig. 1). Its thickness was then reduced 4% by rolling at room temperature. The cold worked tensile specimen was next dead loaded with a stress of 207 MPa, which is approximately ⅓ the yield strength of SMA-23, and cycled from room temperature to ~200°C. During this temperature cycling, the change in specimen length as a function of temperature was measured with an LVDT attached to the specimen grips. As shown in Fig. 7 (data for the 20th cycle), the specimen contracts during the heating part of the cycle and expands during the cooling part. The recoverable strain during each cycle is about 0.7% and the temperature hysteresis is 20-30°C. The temperatures at which the specimen begins to contract and expand correlate reasonably well with the A_s and M_s temperatures obtained by DSC (Fig. 7). Overall, SMA-23 has a reasonably high A_p temperature (~140°C), but rather low recoverable strain.

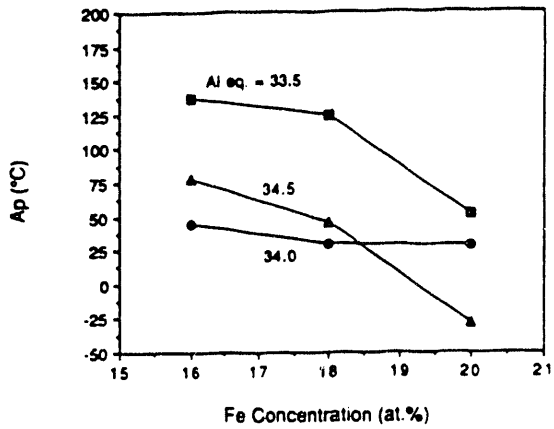

Fig. 4 Effect of Fe on A_p temperatures of Ni-Al-Fe alloys.

SUMMARY AND CONCLUSIONS

Ductility of NiAl-based SMAs can be improved by alloying with B for enhanced grain-boundary cohesion and Fe for improved bulk properties. Fe contents above about 14 at.% are required to get adequate tensile ductilities. Above this level, ductility increases with increasing Fe and Al_{eq}. The phases present in the ductile alloys are martensite, retained B2, and $L1_2$; their relative amounts depend on the exact alloy composition. Elevated temperature exposures (300-500°C) of the ductile alloys result in severe aging-induced embrittlement caused by Ni_5Al_3 precipitation. While Fe improves ductility, it has the deleterious effect that it lowers A_p. For a fixed Fe level, decreasing Al_{eq} increases A_p. At low levels (up to 10 at.%), Mn additions lower A_p, degrade hot workability, and cause room temperature embrittlement. Tensile strain recovery of 0.7% has been achieved in a Ni-Al-Fe alloy with A_p temperature of ~140°C.

ACKNOWLEDGMENTS

The authors thank D. H. Pierce for technical assistance, B. E. Mercer for manuscript preparation, and J. H. Schneibel and C. G. McKamey for manuscript review. This research was sponsored by the Office of Industrial Technologies, Advanced Industrial Concepts Materials Program, and the Division of Materials Sciences, U.S. Department of Energy, under contract DE-AC05-84OR21400 with Martin Marietta Energy Systems, Inc.

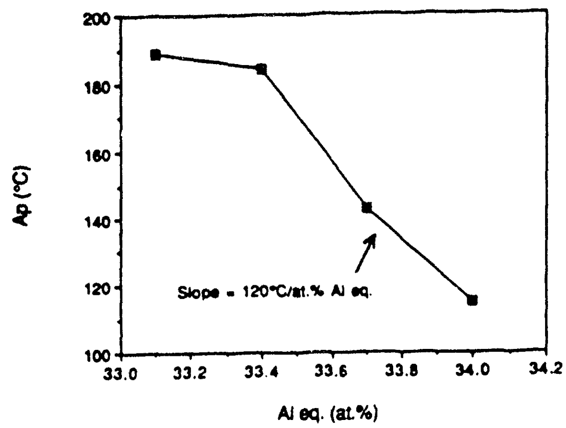

Fig. 5 Effect of Al_{eq} on A_p temperatures of Ni-Al-Fe alloys containing 17.1 at.% Fe.

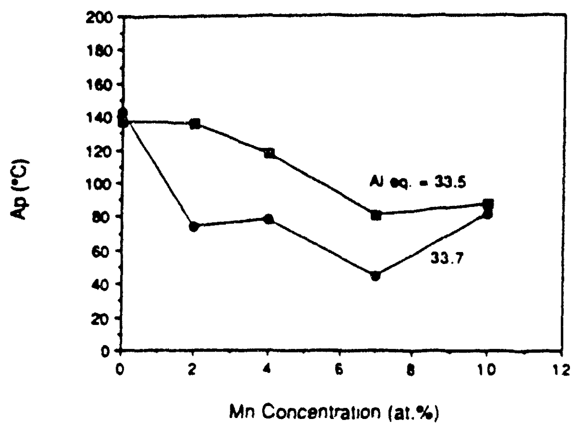

Fig. 6 Effect of Mn on A_p temperatures of Ni-Al-Fe alloys.

REFERENCES

1. R. Kainuma, K. Ishida, and T. Nishizawa, Metall. Trans. **23A**, 1147 (1992).
2. E. P. George, C. T. Liu, C. J. Sparks, Ming-yuan Kao, J. A. Horton, Henry Kunsmann, and Todd King, MRS Symp. Proc. Vol . 246 (1992) p. 121.
3. K. Ishida, R. Kainuma, N. Ueno, and T. Nishizawa, Metall. Trans. **22A**, 441 (1991).
4. Y. D. Kim and C. M. Wayman, Scr. Metall. **25**, 1863-68 (1991).
5. L. E. Tanner, D. Schryvers, and S. M. Shapiro, Mater. Sci. Eng. **A127**, 205-213 (1990).
6. S. Chakravorty and C. M. Wayman, Metall. Trans. **7A**, 555 (1976).
7. S. Chakravorty and C. M. Wayman, Metall. Trans. **7A**, 569 (1976).
8. R. Moskovic, J. Mater. Sci. **12**, 489 (1977).
9. V. S. Litvinov and A. a. Arkhangel's Kaya, Fiz. Met. Metall. **44** (4), 826 (1977).
10. P. Georgopoulos and J. B. Cohen, Scripta Met. **11**, 147 (1977).
11. Y. K. Au and C. M. Wayman, Scripta Metall. **6**, 1209 (1972).
12. J. L. Smialek and R. F. Hehmann, Metall. Trans. **4A**, 1571 (1973).
13. E. P. George and C. T. Liu, J. Mater. Res. **5**, 754 (1990).
14. K. H. Hahn and K. Vedula, Scr. Metall. **23**, 7 (1989).
15. E. P. George, C. T. Liu, and J. J. Liao, MRS Symp. Proc., Vol 186 (1991) p. 375.

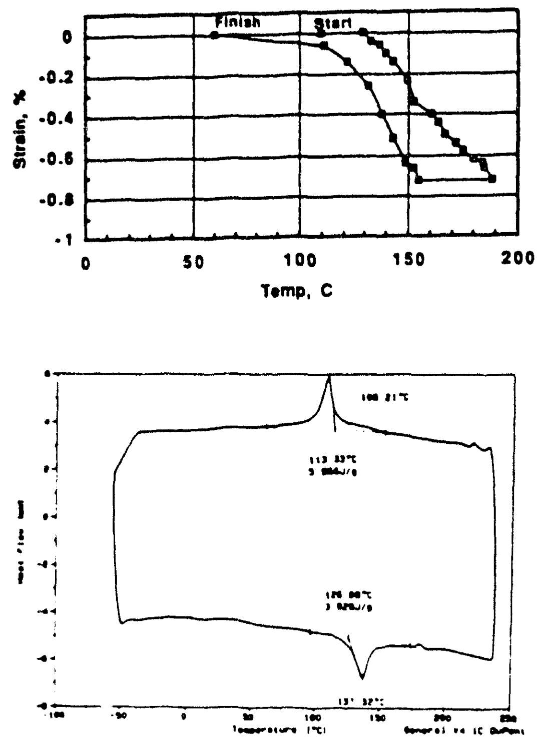

Fig. 7 Tensile strain recovery curve (top), and DSC curve (bottom) of SMA-23.

DATE
FILMED
6 / 28 / 94

END